The Astrophysical Journal, 623:1011–1016, 2005 April 20

THE DIVERSITY OF TYPE Ia SUPERNOVAE: EVIDENCE FOR SYSTEMATICS?

S. Benetti,[1] E. Cappellaro,[2] P. A. Mazzali,[3,4] M. Turatto,[1] G. Altavilla,[5] F. Bufano,[1]
N. Elias-Rosa,[1] R. Kotak,[6] G. Pignata,[7] M. Salvo,[8] and V. Stanishev[9]
Received 2004 October 29; accepted 2004 December 31

ABSTRACT

The photometric and spectroscopic properties of 26 well-observed Type Ia Supernovae (SNe Ia) were analyzed with the aim of exploring SN Ia diversity. The sample includes (Branch) normal SNe, as well as extreme events such as SN 1991T and SN 1991bg, while the truly peculiar SNe Ia, SN 2000cx and SN 2002cx, are not included in our sample. A statistical treatment reveals the existence of three different groups. The first group (FAINT) consists of faint SNe Ia similar to SN 1991bg, with low expansion velocities and rapid evolution of Si II velocity. A second group consists of normal SNe Ia, also with high temporal velocity gradient (HVG), but with brighter mean absolute magnitude $\langle M_B \rangle = -19.3$ and higher expansion velocities than the FAINT SNe. The third group includes both normal and SN 1991T-like SNe Ia: these SNe populate a narrow strip in the Si II velocity evolution plot, with a low-velocity gradient (LVG), but have absolute magnitudes similar to HVGs. While the FAINT and HVG SNe Ia together seem to define a relation between $\mathcal{R}$(Si II) and $\Delta m_{15}(B)$, the LVG SNe either do not conform to that relation or define a new, looser one. The $\mathcal{R}$(Si II) premaximum evolution of HVGs is strikingly different from that of LVGs. We discuss the impact of this evidence on the understanding of SN Ia diversity, in terms of explosion mechanisms, degree of ejecta mixing, and ejecta–circumstellar material interaction.

Subject heading: supernovae: general

Online material: color figures

1. INTRODUCTION

Given the role of Type Ia supernovae (SNe Ia) as distance indicators for cosmology and main producers of heavy elements in the universe, understanding the physics of their explosions and how it influences observables is one of the most fundamental issues in modern astrophysics. One of the keys to penetrate into the secrets of SN Ia physics is to explore the origin of their diversity.

During the last decade, a new paradigm for studying SNe Ia was developed. In particular, a correlation between the peak luminosity and the shape of the early light curve was found, with brighter objects having a slower rate of decline than dimmer ones (Phillips 1993; Phillips et al. 1999, hereafter P99). This is matched by a spectroscopic sequence, defined by the ratio of the depth of two absorption features of Si II at 5972 and 6355 Å (typically observed at 5800 and 6150 Å, respectively; Nugent et al. 1995). This ratio, $\mathcal{R}$(Si II), also correlates with the absolute magnitude of SNe Ia and, in turn, with the rate of decline. Spectral modeling indicates that most of the spectral differences are caused by variations in the effective temperatures, which, in the context of Chandrasekhar-mass explosions, can be interpreted in terms of a variation in the mass of ^{56}Ni produced in the explosions. Alternatively, Garnavich et al. (2004) , using synthetic spectra, tentatively suggest that in SN 1999by and, in general, in SNe Ia with $\Delta m_{15}(B) > 1.2$, the 5800 Å feature is mostly due to Ti II transitions, rather than to Si II.

Although a one-parameter description of SNe Ia has proved to be very useful, it does not completely account for the observed diversity of SNe Ia, (e.g., Benetti et al. 2004; Pignata et al. 2004). Hatano et al. (2000) showed that, contrary to expectations, $\mathcal{R}$(Si II) correlates poorly with the photospheric velocity deduced from the Si II λ6355 absorption. To account for this, they suggested that two or more explosion mechanisms are required to explain SNe Ia variety. Furthermore, some SNe Ia with normal spectra (i.e., showing only lines of typical ions) were noted to show exceptionally high absorption line blueshifts (Branch 1987). Finally, no correlation was found between the blueshift of the Si II λ6355 absorption at the time of maximum brightness and the decline rate parameter, $\Delta m_{15}(B)$, in a small sample of well-observed SNe Ia (see also Patat et al. 1996).

In this paper we further explore this issue, using detailed observations of a large sample of SNe Ia.

2. ANALYSIS

The sample used in this work consists of 26 well-studied SNe Ia. It includes (Branch) normal SNe (Branch et al. 1993) as well as extreme events such as SN 1991T and SN 1991bg, while the truly peculiar SNe Ia, SN 2000cx (Li et al. 2001) and SN 2002cx, (Li et al. 2003) are not included in the sample. Photometric parameters such as $\Delta m_{15}(B)$, extinction, and apparent magnitude at maximum are from P99 or, alternatively, from Altavilla et al. (2004). The spectral parameters have been measured and/or remeasured homogeneously on the available spectra, most of which are published, although unpublished material

[1] INAF-Osservatorio Astronomico, vicolo dell'Osservatorio 5, I-35122 Padova, Italy.
[2] INAF-Osservatorio Astronomico di Capodimonte, via Moiariello 16, I-80131 Napoli, Italy.
[3] INAF-Osservatorio Astronomico, via G. B. Tiepolo 11, I-34131 Trieste, Italy.
[4] Max-Planck-Institut für Astrophysik, Karl-Schwarzschild-Strasse 1, Postfach 1317, D-85741 Garching, Germany.
[5] Departament d'Astronomia i Meteorologia, Universidad de Barcelona, Av. Diagonal 647, E08028 Barcelona, Spain.
[6] Imperial College, Blackett Laboratory, Prince Consort Road, SW7 2AZ London, England, UK.
[7] European Southern Observatory, Karl-Schwarzschild-Strasse 2, D-85748 Garching, Germany.
[8] Research School of Astronomy and Astrophysics, Australian National University, Mount Stromlo Observatory, Cotter Road, Weston Creek, ACT 2611 Canberra, Australia.
[9] Stockholm University, Alba Nova, SE-106 91 Stockholm, Sweden.

TABLE 1

Observed Parameters of the SNe Ia Sample, the Host Galaxies, and References

SN (1)	$\Delta m_{15}(B)$[a] (2)	M_B[b] (3)	$\dot{v}$ (km s^{-1} day^{-1}) (4)	v_{10}(Si II) (1000 km s^{-1}) (5)	$\mathcal{R}$(Si II)$_{max}$[c] (6)	$T_{(RC3)}$ (7)	References (8)
				LVG			
1992A	1.47 ± 0.05	−18.81	67 ± 7	10.83 ± 0.15	0.38 ± 0.05	−1.9	P99, ASA, K93
1989B	1.34 ± 0.07	−18.87	66 ± 5	10.03 ± 0.10	0.29 ± 0.05	3.0	P99, B90, W94
2003kf	1.01 ± 0.05	−19.37	50 ± 5	10.63 ± 0.10	0.18 ± 0.05	3.0	SA05
1996X	1.25 ± 0.05	−19.24	46 ± 5	10.68 ± 0.15	0.25 ± 0.05	−5.0	P99, S01
1999ee	0.94 ± 0.04	−19.46	42 ± 5	9.90 ± 0.10	0.22 ± 0.05	4.0	S02, H02
1990N	1.08 ± 0.05	−19.23	41 ± 5	10.12 ± 0.10	0.21 ± 0.05	3.8	P99, ASA, L91
1994D	1.32 ± 0.05	−19.06	39 ± 5	9.89 ± 0.10	0.33 ± 0.05	−2.0	P99, P96
2003du	1.06 ± 0.06	−18.93	31 ± 5	10.10 ± 0.10	0.22 ± 0.03	8.0	ST05
2001el	1.15 ± 0.04	−18.71	31 ± 5	10.24 ± 0.10	0.30 ± 0.07	5.9	K03, W03, MA05
1997br	1.04 ± 0.15	−19.62	25 ± 5	10.40 ± 0.10	<0.1[d]	7.0	ASA, L99
1999cw	0.94 ± 0.05	−19.24	22 ± 7	10.79 ± 0.15	<0.31[e]	1.5	BU05
1991T	0.95 ± 0.05	−19.62	11 ± 5	9.87 ± 0.10	0.14 ± 0.05	3.8	P99, P92, M95
1998bu	1.04 ± 0.05	−19.12	10 ± 5	10.29 ± 0.10	0.21 ± 0.05	2.0	P99, ASA, H00
				HVG			
1983G	1.37 ± 0.10[g]	−18.62	125 ± 20	13.49 ± 0.20	0.28 ± 0.06	−2.2	H83, B85, T85, B91, B89, McDA
2002bo	1.17 ± 0.05	−19.42	110 ± 7	11.73 ± 0.15	0.17 ± 0.05	1.0	B04
1997bp	1.09 ± 0.10	−19.69	106 ± 7	13.87 ± 0.20	0.16 ± 0.05	[f]	A04, ASA
2002er	1.33 ± 0.04	−19.45	92 ± 5	10.52 ± 0.10	0.23 ± 0.05	1.0	P04, KO05
1984A	1.21 ± 0.10[g]	−19.46	92 ± 10	12.64 ± 0.15	0.23 ± 0.05	1.0	B89, Ba89, W87, McDA
1989A	1.06 ± 0.10[g]	−19.21	90 ± 10	12.13 ± 0.15	0.22 ± 0.07	4.1	B91, McDA
2002dj	1.12 ± 0.05	−19.05	86 ± 6	12.18 ± 0.10	0.17 ± 0.05	−5.0	PI05
1981B	1.11 ± 0.07	−19.21	76 ± 7	11.11 ± 0.15	0.16 ± 0.05	4.5	P99, B83
				FAINT			
1999by	1.87 ± 0.10	−16.64	110 ± 10	9.06 ± 0.10	0.58 ± 0.06	3.0	B99, V01, H01
1991bg	1.93 ± 0.10	−16.81	104 ± 7	8.50 ± 0.15	0.62 ± 0.05	−4.7	P99, T96
1997cn	1.86 ± 0.10	−16.95	83 ± 10	8.81 ± 0.20	0.63 ± 0.06	−5.0	T98
1993H	1.70 ± 0.10	−18.20	73 ± 8	10.10 ± 0.20	0.52 ± 0.05	1.9	P99, ASA, CTIO
1986G	1.78 ± 0.07	−17.48	64 ± 5	9.36 ± 0.15	0.53 ± 0.05	−2.2	P99, P87, C92

[a] Reddening corrected according to P99.

[b] Cepheids distances taken from Altavilla et al. (2004; $H_0 = 72$ km s^{-1} Mpc^{-1}) when available; otherwise, relative distances to Virgo taken from Kraan-Korteweg (1986) and a Virgo distance of 15.3 Mpc (Freedman et al. 2001) or from Hubble flow.

[c] Measured at maximum light.

[d] Si II λ5972 not visible on the -3^d spectrum; spectra close to maximum not available.

[e] Measured on the earliest available spectrum ($\phi = +5d$).

[f] Irregular galaxy.

[g] Determination of $\Delta m_{15}(B)$ from published data.

References.—(A04) Altavilla et al. 2004; (ASA) Asiago supernova archive; (B04) Benetti et al. 2004; (B83) Branch et al. 1983; (B85) Buta et al. 1985; (B89) Benetti 1989; (B90) Barbon et al. 1990; (B91) Benetti et al. 1991; (B99) Bonanos et al. 1999; (Ba89) Barbon et al. 1989; (BU05) Bufano et al. 2005, in preparation; (C92) Cristiani et al. 1992; (CTIO) Cerro Tololo Inter-American Observatory archive; (H00) Hernandez et al. 2000; (H01) Howell et al. 2001; (H02) Hamuy et al. 2002; (H83) Harris et al. 1983; (K03) Krisciunas et al. 2003; (K93) Kirshner et al. 1993; (KO05) Kotak et al. 2005; (L91) Leibundgut et al. 1991; (L99) Li et al. 1999; (M95) Mazzali et al. 1995; (MA05) Mattila et al. 2005, in preparation; (McDA) McDonald archive; (P04) Pignata et al. 2004; (P87) Phillips et al. 1987; (P92) Phillips et al. 1992; (P96) Patat et al. 1996; (P99) Phillips et al. 1999; (PI05) Pignata et al. 2005, in preparation; (S01) Salvo et al. 2001; (S02) Stritzinger et al. 2002; (SA05) Salvo et al. 2005, in preparation; (ST05) Stanishev et al. 2005, in preparation; (T85) Tsvetkov 1985; (T96) Turatto et al. 1996; (T98) Turatto et al. 1998; (V01) Vinko et al. 2001; (W03) Wang et al. 2003; (W87) Wegner & McMahan 1987; (W94) Wells et al. 1994.

collected in the Asiago Supernova Archive (ASA) by the Padua-Asiago SN group and the European Supernova Collaboration was also used. In Table 1 we summarize the main photometric and spectroscopic parameters of the SNe Ia sample, together with the morphological type (T) of the host galaxy as given in the Third Reference Catalog of Bright Galaxies (RC3). The SNe are divided into three groups according to the criteria discussed in § 2.1. In each group the SNe are arranged by decreasing $\dot{v}$ (see § 2.1).

2.1. *Expansion Velocities from* Si II

The expansion velocity of the ejecta gives a direct indication of the kinetic energy of the explosion. The blueshift of the Si II λ6355 absorption, the most prominent line in the photospheric phase spectrum, traces the evolution of the expansion velocity of the ejecta over the first 4–5 weeks past explosion. A plot of the time evolution of the expansion velocity, v(Si) for the SNe Ia of our sample (Fig. 1) confirms the results of Branch (1987). At any given phase, expansion velocities span a wide range of ~4000 km s^{-1}, from the very rapidly expanding ejecta of SN 1983G and SN 1997bp to the low velocity, SN 1991bg-like events. Between these limits, both the normal SNe Ia and the luminous SN 1991T-like events are found. A convenient parameter to distinguish different SNe Ia is the expansion velocity measured 10 days past maximum, v_{10}(Si II). As we mentioned earlier, this parameter

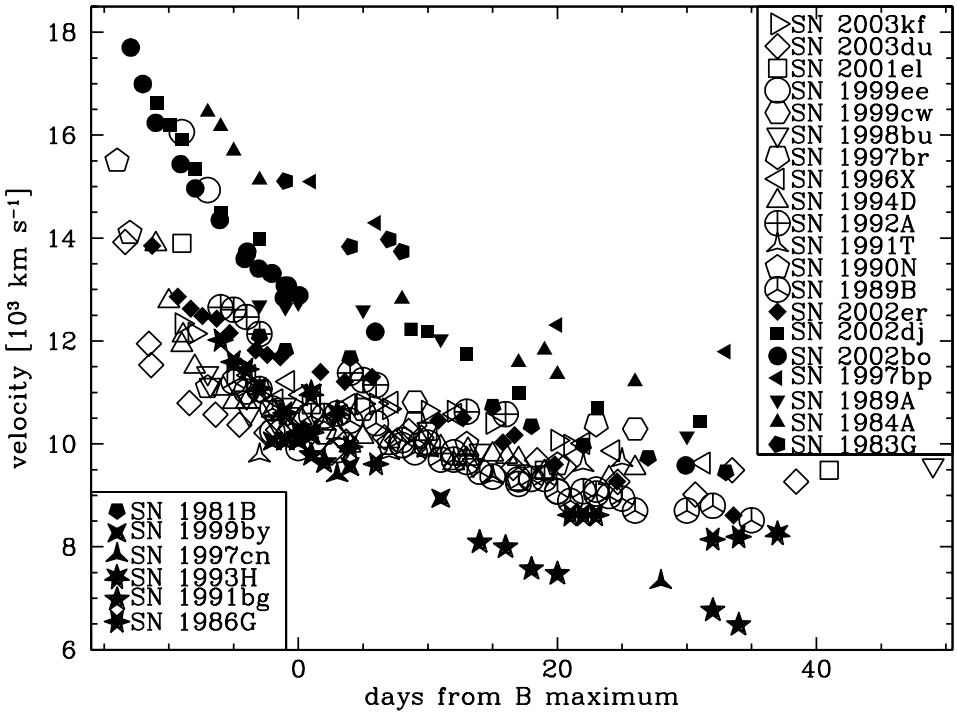

FIG. 1.—Time evolution of the photospheric velocity derived from Si II λ6355 for the SNe of Table 1. The filled symbols refer to HVG, open symbols to LVG, and starred to FAINT SNe Ia. [*See the electronic edition of the Journal for a color version of this figure.*]

correlates poorly with $\mathcal{R}$(Si II) (Hatano et al. 2000) or with $\Delta m_{15}(B)$ (Patat et al. 1996); hence it may give interesting clues regarding the origin of SN Ia diversity.

Upon more careful scrutiny, and thanks to the excellent coverage offered by the new data, it can be noted that the velocities show not only a spread in value, but a significant difference in velocity evolution. In particular, a subgroup of very homogeneous SNe Ia, characterized by a shallow evolution of the expansion velocity (Fig. 1; *open symbols*), populates a narrow strip in the postmaximum velocity evolution diagram. For a quantitative analysis, we introduce a new parameter, $\dot{v} = -\Delta v/\Delta t$, which is the average daily rate of decrease of the expansion velocity (Table 1, col. [4]). This is derived from least-squares fits of the measurements taken between maximum and either the time the Si II feature disappears or the last available spectrum, whichever is earlier.

On average, the LVG SNe Ia have a velocity gradient $\dot{v} < 60-70$ km s^{-1} day^{-1}. The SNe Ia shown as filled symbols (Fig. 1) have a larger $\dot{v} > 70$ km s^{-1} day^{-1}, reaching 110–125 km s^{-1} day^{-1} for SN 2002bo, SN 1991bg, and SN 1983G (although the value for SN 1983G is quite uncertain).

A similar dichotomy in velocity slopes between SNe Ia can be found in the velocities deduced from the S II λ5640 line, this time at premaximum phases (see Fig. 11 of Benetti et al. 2004).

For an objective identification of possibly homogeneous groups, we performed a hierarchical cluster analysis for the SN Ia sample of Table 1, considering both photometric and spectroscopic parameters, but neglecting the dependence on galaxy morphological type. Hierarchical cluster analysis (Anderberg 1973) is an exploratory data analysis tool that aims to identify relatively homogeneous groups of events based on selected characteristics using an algorithm that starts with each case in a separate cluster and combines clusters until only one is left. Cluster analysis simply discovers structures in data without explaining why they exist. The choice of the number of clusters to be considered is somewhat arbitrary, although a criterion is the distance of the groups in the parameter space. Indeed, in the five dimensions space, we found three well-separated clusters:

1. A first cluster (FAINT) consists of faint SNe Ia, with $\langle M_B \rangle = -17.2$ ($\sigma = 0.6$), similar to SN 1991bg. All these SNe have a high postmaximum luminosity decline rate, $\langle \Delta m_{15}(B) \rangle = 1.83$ ($\sigma = 0.09$), and Si II line ratio, $\langle \mathcal{R}(\text{Si II}) \rangle = 0.58$ ($\sigma = 0.05$). They have small expansion velocities, $\langle v_{10}(\text{Si II}) \rangle = 9.2$ ($\sigma = 0.6$), and a large velocity gradient, $\langle \dot{v} \rangle = 87$ ($\sigma = 20$).
2. A second group consists of normal SNe Ia with HVG, $\langle \dot{v} \rangle = 97$ ($\sigma = 16$). These SNe have average absolute magnitude $\langle M_B \rangle = -19.3$ ($\sigma = 0.3$), $\Delta m_{15}(B) = 1.2$ ($\sigma = 0.1$), and $\langle \mathcal{R}(\text{Si II}) \rangle = 0.20$ ($\sigma = 0.05$). They typically have high expansion velocities, $\langle v_{10}(\text{Si II}) \rangle = 12.2$ ($\sigma = 1.1$).
3. A third group consists of SNe with LVG, $\langle \dot{v} \rangle = 37$ ($\sigma = 18$), but it includes both normal SNe Ia and all the brightest SNe. Although its postmaximum decline rate is somewhat slower than that of the HVG SNe, $\langle \Delta m_{15}(B) \rangle = 1.1$ ($\sigma = 0.2$), its average luminosity is similar, $\langle M_B \rangle = -19.2$ ($\sigma = 0.3$), and so is their $\langle \mathcal{R}(\text{Si II}) \rangle = 0.25$ ($\sigma = 0.07$). On average, the LVG SNe have lower and more homogeneous expansion velocities than the HVG SNe, $\langle v_{10}(\text{Si II}) \rangle = 10.3$ ($\sigma = 0.3$).

For a few events, in particular SN 1989B and SN 1992A, cluster membership is uncertain. A small variation of the parameters, still within the errors, could shift them from the LVG to the HVG group.

It is also interesting that, on average, the host galaxy morphological type is progressively later as one moves from FAINT to HVG and to LVG. The average values are −1.4, 0.6, and 2.5, respectively. The dispersion within each group is, however, very large ($\sigma = 3-4$). This is consistent with the finding that bright SNe Ia occur preferentially in late-type galaxies, while faint SNe Ia are more often found in early-type galaxies (Altavilla et al. 2004).

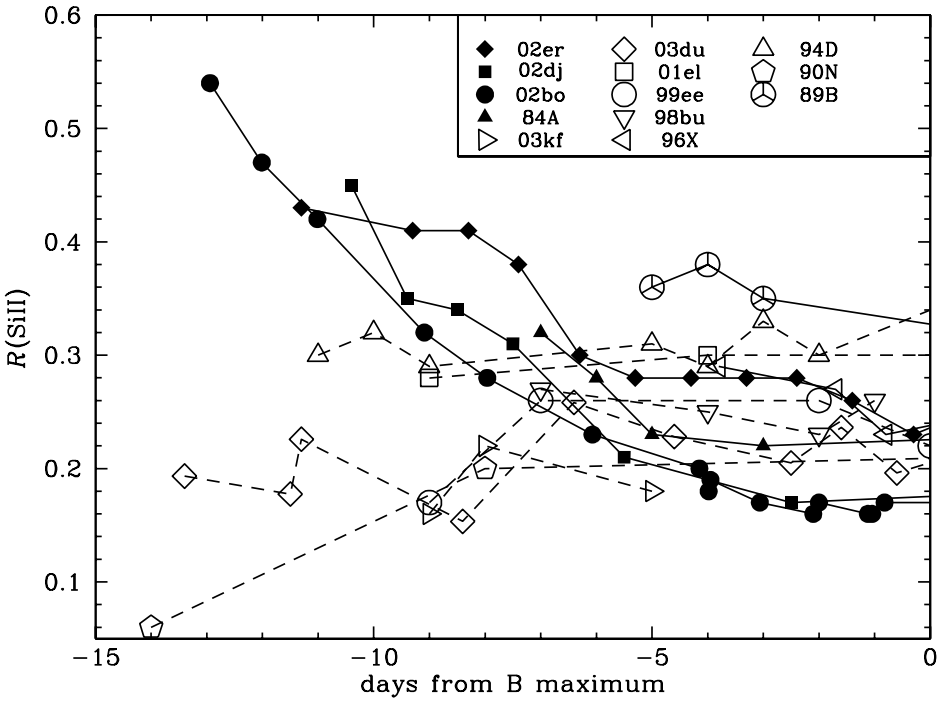

FIG. 2.—Premaximum temporal evolution of the $\mathcal{R}$(Si II) parameter for our sample of SNe Ia. Symbols are as in Fig. 1. [*See the electronic edition of the Journal for a color version of this figure.*]

2.2. *Premaximum Evolution of* $\mathcal{R}$(Si II)

Figure 2 shows the premaximum evolution of $\mathcal{R}$(Si II) for our sample of SNe Ia. Interestingly, the HVG SNe Ia for which very early observations are available show a dramatic temporal evolution of $\mathcal{R}$(Si II), starting from a high value well before maximum and leveling out just before maximum, as was the case for SN 2002bo (Benetti et al. 2004). On the other hand, the LVG SNe show on average either no evolution in $\mathcal{R}$(Si II) before maximum or an evolution in the opposite sense in the case of SN 1990N. Clearly, the number of SNe Ia for which very early spectra are available is still too small to draw definite conclusions, but it is worth speculating on a possible interpretation.

Since $\mathcal{R}$(Si II) is related to the photospheric temperature of the ejecta (Nugent et al. 1995), the curves in Figure 2 should trace the temperature evolution in the line-forming regions before maximum light. HVG SNe seem to start at cooler temperatures, which then increase approaching maximum. LVG SNe, on the other hand, have high temperatures already well before maximum. This may be related to the fact that LVG SNe have lower expansion velocities, especially before maximum, and are also hotter.

2.3. $\mathcal{R}(\text{Si II})_{\max}$ *versus* $\Delta m_{15}(B)$

In Figure 3*a*, the value of $\mathcal{R}(\text{Si II})_{\max}$ measured for each SN Ia at maximum light is plotted against $\Delta m_{15}(B)$. SNe in both the FAINT and HVG groups seem to follow the relation between $\mathcal{R}(\text{Si II})_{\max}$ and $\Delta m_{15}(B)$ established by Nugent et al. (1995). LVG SNe, on the other hand, are more scattered in this plot, especially at the bright, slow end. Either they do not conform with the $\mathcal{R}(\text{Si II})_{\max} - \Delta m_{15}(B)$ relation, or they define a new, looser one.

The scatter of LVG SNe in Figure 3*a*, especially at low $\Delta m_{15}(B)$, suggests that another physical parameter besides the temperature is needed to describe their behavior. Garnavich et al. (2004), using SYNOW synthetic spectra, tentatively suggest that

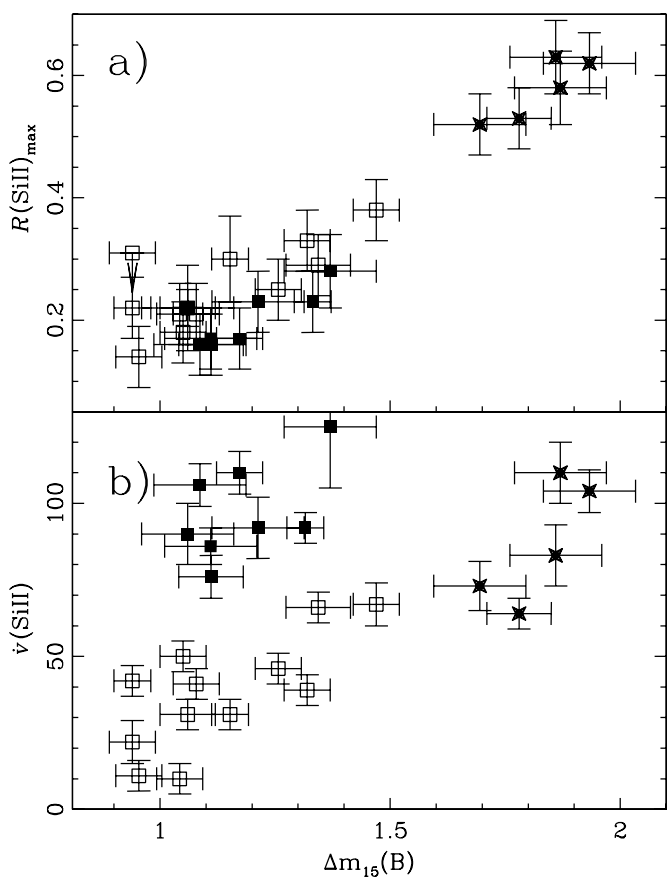

FIG. 3.—(*a*) $\Delta m_{15}(B)$ vs. $\mathcal{R}(\text{Si II})_{\max}$ for the SNe of our sample. (*b*) $\Delta m_{15}(B)$ vs. $\dot{v}$ of Si II λ6355. Open symbols show LVG SNe, filled symbols show HVG SNe, and starred symbols show FAINT SNe. [*See the electronic edition of the Journal for a color version of this figure.*]

in SN 1999by and, in general, in SNe Ia with $\Delta m_{15}(B) > 1.2$, the 5800 Å feature is mostly due to Ti II transitions rather than to Si II, and claim that only with this interpretation can the $\mathcal{R}(\text{Si II})_{\max} - \Delta m_{15}(B)$ relation be understood. However, neither our synthetic spectral analysis of SN 1991bg (Mazzali et al. 1997) nor the spectral tomography analysis of the normal SN Ia, SN 2002bo, exploring a wide range of photospheric temperatures and chemical compositions (Stehle et al. 2004), requires a relevant contribution from the Ti II transitions to fit the 5800 Å feature. Indeed, in the above-mentioned models, the 5800 Å feature is always well fitted by the Si II 5972 Å transition. As for the SNe Ia with $\Delta m_{15}(B) < 1.2$, Garnavich et al. (2004) confirm that the 5800 Å feature is indeed Si II.

2.4. $\dot{v}$ *versus* $\Delta m_{15}(B)$

The $\Delta m_{15}(B)$ parameter is plotted versus $\dot{v}$ in Figure 3*b*. The expansion velocity evolution gradient, $\dot{v}$, seems to be weakly correlated with $\Delta m_{15}(B)$: while SNe with a large $\Delta m_{15}(B)$ (the FAINT group) have a large $\dot{v}$, normal SNe can have both a large or a small $\dot{v}$. Cluster analysis, however, suggests that we are dealing with three distinct families of SNe Ia: FAINT, LVG, and HVG. These three groups may be characterized by different physical parameters governing the same explosion mechanism (possibly distinguishing LVG and HVG) or by a totally different kind of explosion, which may be more likely for the FAINT group.

3. DISCUSSION

Based on the evidence presented above, we can make a preliminary attempt to explain the causes of the spectroscopic diversity among SNe Ia.

As Figures 1, 2, and 3 show, SNe Ia can be divided into three groups. Each group has distinct physical properties, different from those of other groups. In particular, the FAINT group (essentially the SN 1991bg-like objects, plus SN 1986G and SN 1993H according to this method; but see Meikle [2000] for an infrared view) clearly differs from the other two: these SNe are fast decliners in both luminosity and velocity, and they have typically low velocities and occur in earlier-type galaxies. This may not be surprising, since in many ways SN 1991bg-like objects stand out as odd.

For the other two groups, the situation is more complicated: both HVG and LVG include normal SNe, but the LVG also include all the brightest, slowest declining SNe. Our analysis suggests that LVG and HVG are two distinct groups, but they may possibly represent a continuum of properties.

Interestingly, although it is common to refer to two main groups of peculiar SNe Ia, SN 1991bg-like and SN 1991T-like, the latter SNe fall in the same class as normal SNe, while the former do not. There appears to be a discontinuity of properties between SN 1991bg-like objects and all other SNe Ia, which is not seen for SN 1991T-like SNe. This is not what we might expect if SNe Ia behaved as a simple one-parameter family of events.

Based on a qualitative analysis, Benetti et al. (2004) suggested that the large blueshift of the Si II line in SN 2002bo (a HVG SN) maybe the result of a delayed-detonation explosion. Moreover, Lentz et al. (2000) find, from detailed non-LTE calculations, that some delayed-detonation models can account for the very high Si II blueshift of another HVG, SN 1984A. It may be that the HVG SNe are delayed detonations, their internal dispersion arising from a range of transition densities, while the LVG SNe are deflagrations. This would be an extension of the results of Hatano et al. (2000; see their Fig. 1). The only difference from their conclusions would be that SN 1981B and SN 1992A would become a delayed detonation and a deflagration event, respectively. From spectropolarimetric studies, Wang et al. (2004) also reached the conclusion that the explosion mechanism of SN 1984A, SN 1997bp, SN 2002bo, (all HVG SNe) and SN 2004dt, which is most probably also a HVG SN, may be markedly different from that of lower velocity objects such as SN 1994D.

The LVG SNe include all three SNe in our sample with $\Delta m_{15}(B) < 1$: SN 1991T, SN 1999cw, and SN 1999ee. SN 1991T has also often been discussed as the result of a delayed detonation, especially in order to explain the high abundance of ^{56}Ni and its decay products at the highest velocities (Mazzali et al. 1995), so its inclusion in the LVG does not support the hypothesis that all LVG SNe are deflagrations. Very early measurements of v(Si) are not possible for SN 1991T, since the Si II line was almost absent in the earliest spectra, owing to the high degree of ionization. The photospheric velocities inferred from spectral models were, however, very high (Mazzali et al. 1995). This might support the suggestion made by Wang et al. (2004) that SN 1991T-like events could be SN 1984A-like events viewed at different angles (and thus HVGs).

Differences in the properties of the outer ejecta, such as a different degrees of mixing, or of circumstellar interaction, may also be at the origin of the difference between LVG and HVG.

More efficient mixing out of heavy elements might result in an initially higher photospheric velocity. At the earliest times, the photosphere should in fact tend to trace the heavier elements, since they have much larger line opacity, and this is the major contributor to the optical depth (Pauldrach et al. 1996). The initial rate of decrease of the velocity with time would consequently be larger, as the photosphere moves inward to layers that are not so different from those of less-mixed SNe. This would also mean a temperature initially lower (resulting from the large photosphere) but increasing with time. This would be the HVG group.

On the other hand, less efficient mixing could lead to initially smaller photospheric velocities: light elements contribute much less to the opacity, and thus the photosphere would be deeper and the premaximum temperature higher. The decline rate of the velocity would then be smaller, and the temperature would either stay constant or decline, depending on the exact combination of increasing luminosity and decreasing photospheric velocity. These are the properties of the LVG.

Very high velocity features have been observed in all SNe with sufficiently early spectra (Mazzali et al. 2005b). Perhaps in the LVG, the interaction affects the spectra only very early, as in SN 1999ee (Mazzali et al. 2005a) or SN 1990N (Fisher et al. 1997; Mazzali 2001), and there is a sudden drop to lower velocities when the interaction ends, resulting in a lower post-maximum $\dot{v}$, while it continues for a longer time in the HVG, so that v_{10}(Si II) spans a broader range of values.

In both of these last scenarios, LVG and HVG SNe would not necessarily be differentiated by the nature of the explosion, and they may even represent a continuum of properties.

We are in debt to J. Sollerman, P. Lundqvist, M. M. Phillips, S. Mattila, and J. C. Wheeler for providing us unpublished SNe spectra. We also acknowledge D. A. Howell and L. Wang for sending us the spectra of SN 1999by and SN 2001el, respectively. This work is supported in part by the European Community's Human Potential Programme under contract HPRN-CT-2002-00303, "The Physics of Type Ia Supernovae."

REFERENCES

Altavilla, G., et al. 2004, MNRAS, 349, 1344 (A04)
Anderberg, M. R. 1973, Cluster Analysis for Applications (New York: Academic Press)
Barbon, R., Benetti, S., Rosino, L., Cappellaro, E., & Turatto, M. 1990, A&A, 237, 79 (B90)
Barbon, R., Rosino, L., & Iijima, T. 1989, A&A, 220, 83 (Ba89)
Benetti, S. 1989, Ph.D. thesis, Universitá di Padova (B89)
Benetti, S., Cappellaro, E., & Turatto, M. 1991, A&A, 247, 410 (B91)
Benetti, S., et al. 2004, MNRAS, 348, 261 (B04)
Bonanos, A., Garnavich, P., Schlegel, E., Jha, S., Challis, P., Kirshner, R., Hatano, K., & Branch, D. 1999, BAAS, 31, 1424 (B99)
Branch, D. 1987, ApJ, 316, L81
Branch, D., Fisher, A., & Nugent, P. 1993, AJ, 106, 2383
Branch, D., Lacy, C. H., McCall, M. L., Sutherland, P. G., Uomoto, A., Wheeler, J. C., & Wills, B. J. 1983, ApJ, 270, 123 (B83)
Buta, R. J., Corwin, H. G., & Opal, C. B. 1985, PASP, 97, 229 (B85)
Cristiani, S., et al. 1992, A&A, 259, 63 (C92)
Fisher, A., Branch, D., Nugent, P., & Baron, E. 1997, ApJ, 481, L89
Freedman, W. L., et al. 2001, ApJ, 553, 47
Garnavich, P. M., et al. 2004, ApJ, 613, 1120
Hamuy, M., et al. 2002, AJ, 124, 2339 (H02)
Harris, G. L., Hesser, J. E., Massey, P., Peterson, C. J., & Yamanaka, J. M. 1983, PASP, 95, 607 (H83)
Hatano, K., Branch, D., Lentz, E. J., Baron, E., Filippenko, A. V., & Garnavich, P. M. 2000, ApJ, 543, L49
Hernandez, M., et al. 2000, MNRAS, 319, 223 (H00)
Howell, D. A., Höflich, P., Wang, L., & Wheeler, J. C. 2001, ApJ, 556, 302 (H01)
Kirshner, R. P., et al. 1993, ApJ, 415, 589 (K93)
Kotak, R., et al. 2005, MNRAS, submitted (KO05)
Kraan-Korteweg, R. C. 1986, A&AS, 66, 255
Krisciunas, K., et al. 2003, AJ, 125, 166 (K03)
Leibundgut, B., Kirshner, R. P., Filippenko, A. V., Shields, J. C., Foltz, C. B., Phillips, M. M., & Sonneborn, G. 1991, ApJ, 371, L23 (L91)
Lentz, E. J., Baron, E., Branch, D., Hauschildt, P. H., & Nugent, P. E. 2000, ApJ, 530, 966
Li, W., et al. 2001, PASP, 113, 1178
———. 2003, PASP, 115, 453
Li, W. D., et al. 1999, AJ, 117, 2709 (L99)
Mazzali, P. A. 2001, MNRAS, 321, 341
Mazzali, P. A., Benetti, S., Stehle, M., Branch, D., Deng, J., Maeda, K., Nomoto, K., & Hamuy, M. 2005a, MNRAS, 357, 200
Mazzali, P. A., Chugai, N., Turatto, M., Lucy, L. B., Danziger, I. J., Cappellaro, E., della Valle, M., & Benetti, S. 1997, MNRAS, 284, 151
Mazzali, P. A., Danziger, I. J., & Turatto, M. 1995, A&A, 297, 509 (M95)
Mazzali, P. A., et al. 2005b, ApJ, 623, L37
Meikle, W. P. S. 2000, MNRAS, 314, 782
Nugent, P., Phillips, M., Baron, E., Branch, D., & Hauschildt, P. 1995, ApJ, 455, L147
Patat, F., Benetti, S., Cappellaro, E., Danziger, I. J., della Valle, M., Mazzali, P. A., & Turatto, M. 1996, MNRAS, 278, 111 (P96)
Pauldrach, A. W. A., Duschinger, M., Mazzali, P. A., Puls, J., Lennon, M., & Miller, D. L. 1996, A&A, 312, 525
Phillips, M. M. 1993, ApJ, 413, L105
Phillips, M. M., Lira, P., Suntzeff, N. B., Schommer, R. A., Hamuy, M., & Maza, J. 1999, AJ, 118, 1766 (P99)
Phillips, M. M., Wells, L. A., Suntzeff, N. B., Hamuy, M., Leibundgut, B., Kirshner, R. P., & Foltz, C. B. 1992, AJ, 103, 1632 (P92)
Phillips, M. M., et al. 1987, PASP, 99, 592 (P87)
Pignata, G., et al. 2004, MNRAS, 355, 178 (P04)
Salvo, M. E., Cappellaro, E., Mazzali, P. A., Benetti, S., Danziger, I. J., Patat, F., & Turatto, M. 2001, MNRAS, 321, 254 (S01)
Stehle, M., Mazzali, P. A., Benetti, S., Hillebrandt, W. 2004, MNRAS, submited (astro-ph/0409342)
Stritzinger, M., et al. 2002, AJ, 124, 2100 (S02)
Tsvetkov, D. Y. 1985, Soviet Astron., 29, 211 (T85)
Turatto, M., Benetti, S., Cappellaro, E., Danziger, I. J., della Valle, M., Gouiffes, C., Mazzali, P. A., & Patat, F. 1996, MNRAS, 283, 1 (T96)
Turatto, M., Piemonte, A., Benetti, S., Cappellaro, E., Mazzali, P. A., Danziger, I. J., & Patat, F. 1998, AJ, 116, 2431 (T98)
Vinkó, J., Kiss, L. L., Csák, B., Fűrész, G., Szabó, R., Thomson, J. R., & Mochnacki, S. W. 2001, AJ, 121, 3127
Wang, L., Baade, D., Hoeflich, P., Wheeler, J. C., Kawabata, K., Khokhlov, A., Nomoto, K., & Patat, F. 2004, ApJ, submitted (astro-ph/0409593)
Wang, L., et al. 2003, ApJ, 591, 1110 (W03)
Wegner, G., & McMahan, R. K. 1987, AJ, 93, 287 (W87)
Wells, L. A., et al. 1994, AJ, 108, 2233 (W94)